Nano Research 2017, 10(5): 1840–1846
DOI 10.1007/s12274-017-1548-9
Research Article
ISSN 1998-0124
CN 11-5974/O4

Near-infrared light activated persistent luminescence nanoparticles via upconversion

Zhanjun Li[1,2], Ling Huang[1], Yuanwei Zhang[1], Yang Zhao[1], Hong Yang[1], and Gang Han[1] (✉)

[1] *Department of Biochemistry and Molecular Pharmacology, University of Massachusetts Medical School, Worcester, Massachusetts 01605, USA*
[2] *School of Environment, Jinan University, Guangzhou 510630, China*

Received: 12 January 2017
Revised: 21 February 2017
Accepted: 21 February 2017

KEYWORDS
nanoparticles,
imaging,
persistent luminescence,
upconversion

ABSTRACT

Persistent luminescence nanoparticles (PLNPs) and upconversion nanoparticles (UCNPs) are two special optical imaging nanoprobes. In this study, efficient upconverted persistent luminescence (UCPL) is realized by combining their unique features into polymethyl methacrylate, forming a film composed of both PLNPs and UCNPs. The red persistent luminescence (~640 nm) of the PLNPs (CaS:Eu,Tm,Ce) can be activated by upconverted green emission of UCNPs (β-$NaYF_4$:Yb,Er@$NaYF_4$) excited by near-infrared light (NIR). Using this strategy, both the unique optical properties of PLNPs and UCNPs can be optimally synergized, thus generating efficient upconversion, photoluminescence, and UCPL simultaneously. The UCPL system has potential applications in *in vivo* bioimaging by simply monitoring the biocompatible low power density of NIR-light-excited persistent luminescence. Due to its simplicity, we anticipate that this method for the preparation of UCPL composite can be easily adjusted using other available upconversion and persistent phosphor pairs for a number of biophotonic and photonic applications.

1 Introduction

Persistent luminescence (PL) is the afterglow emission of phosphors after excitation ceases [1, 2], which allows complete separation of the excitation and emission processes. Utilizing this unique property of persistent luminescence nanoparticles (PLNPs), high-quality *in vivo* luminescence imaging is possible owing to the absence of auto-fluorescence [3]. This has led to the creation of a great number of new persistent phosphors [4–12]. Much effort has been spent on exploring the diverse applications of PLNPs, such as in targeted tumor PL imaging [13], multi-model imaging [14, 15], traceable drug delivery [16, 17], cell tracking [18], bio-sensing [19], analysis [20, 21], and even new energy source exploration [22]. However, *in vitro* pre-excitation is typically needed to efficiently charge the PLNPs, in which some of the excitation energy is stored in the so-called energy traps and thereafter gradually released in order to generate PL.

Address correspondence to Gang.Han@umassmed.edu

After the stored energy is exhausted, the PL process ceases. Although a photo-stimulated PL strategy can be used to partially recover the exhausted PL in certain PLNPs (such as $LiGa_5O_8$:Cr), *in vivo* reactivation is needed to satisfy the needs of long-term imaging applications [23]. The visible-light-activating properties of $ZnGa_2O_4$:Cr (a typical persistent phosphor at 700 nm) were found to be useful for achieving real-time PL imaging both *in situ* and *in vivo* [24–26]. However, the PL of $ZnGa_2O_4$:Cr is most efficiently excited by ultraviolet (UV) light due to the large band gap of $ZnGa_2O_4$ (4.4 eV) [27–29]. In contrast, its PL, when excited by visible light derived from the absorption of Cr, is much weaker than that excited by UV light, which limits its potential clinical application at the deep tissue level because of the relatively poor transparency of bio-tissue with respect to UV/visible light [30]. Near-infrared (NIR) light is frequently used in photodynamic and photothermal therapy because of the well-known NIR biological window (~650 to ~1,000 nm). Pan et al. reported the first upconverted persistent phosphor, $Zn_3Ga_2GeO_8$:Cr^{3+},Yb^{3+},Er^{3+}, which can be activated by a near-infrared laser (980 nm) and is able to emit long-lasting PL that peaks at 700 nm [31]. Despite this demonstration of the upconverted persistent luminescence (UCPL) concept in bulk materials, a few limitations have hampered the development of such materials for *in vivo* study. For example, the doping of Yb/Er greatly decreased the PL. Further, $Zn_3Ga_2GeO_8$ is a good matrix for persistent phosphors but is not an ideal matrix for doping Yb/Er for upconversion (UC) [32–35]. Its relatively low upconversion efficiency is likely, in turn, to reduce the efficiency of the UCPL process. Therefore, it is desirable to design an upconverted PLNP system that has excellent PL/UC/UCPL composite properties while largely retaining each luminescence modality.

Since a classic deep red (peaking at 640 nm) persistent phosphor, CaS:Eu^{2+},Tm^{3+},Ce^{3+}, can be efficiently excited by visible light that overlaps well with the efficient green upconversion of classical β-$NaYF_4$:Yb,Er/$NaYF_4$ nanoparticles (Fig. S1 in the Electronic Supplementary Material (ESM)) [36, 37], we hypothesize that efficient UCPL can be realized by integrating these two efficient PL and upconversion nanoparticles (UCNPs) (Scheme 1). Under 980 nm laser irradiation,

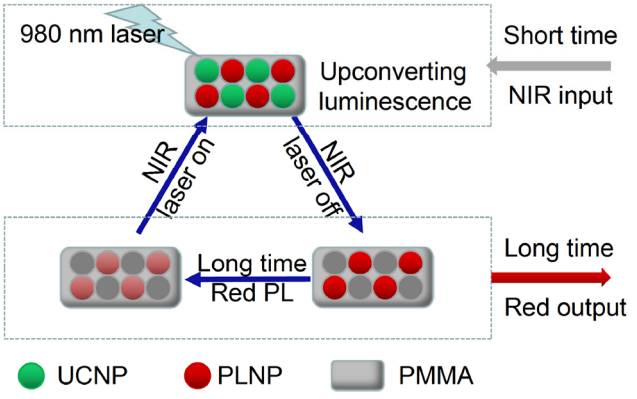

Scheme 1 A schematic illustration of a NIR-in/long-time-red-out UCPL system.

intense green UC can be generated, and this activates the nearby PLNPs. Although the UC luminescence ceases right after turning off the NIR laser, the efficient red PL is maintained for a long period. Once the stored energy is exhausted, the red PL can be recharged by a NIR laser. Thus, an efficient UCPL composite film was developed to achieve long-period deep red PL after brief NIR laser irradiation.

2 Results and discussion

In this study, we synthesized CaS:0.02%Eu,0.1%Tm, 0.1%Ce, PLNPs, and β-$NaYF_4$:Yb,Er@$NaYF_4$, UCNPs (Figs. 1(a) and 1(b)) according to previous research [37, 38]. The PL excitation spectra of CaS:Eu,Tm,Ce indicate that its PL peaks at 640 nm and that this can be efficiently excited by the 540 nm upconversion luminescence of the as-synthesized β-$NaYF_4$:Yb,Er@$NaYF_4$ nanoparticles (Fig. 2). The synthesized PLNPs and UCNPs were subsequently dispersed into polymethyl methacrylate (PMMA)/dichloromethane solution. After the dichloromethane evaporated, the nanophosphors were embedded into PMMA forming a UCPL thin film, as shown in Fig. 1(c). Under 980 nm constant wave laser excitation, intense green emission can be generated. After turning off the laser, deep red PL can be easily observed by the naked eye in the dark. The UCPL film also inherited the intense afterglow property of the PLNPs after white light LED excitation. Thus, 3-in-1 UC/PL/UCPL films were successfully obtained (Fig. 1(c)).

Figure 3(a) shows the UC spectra of the UCPL

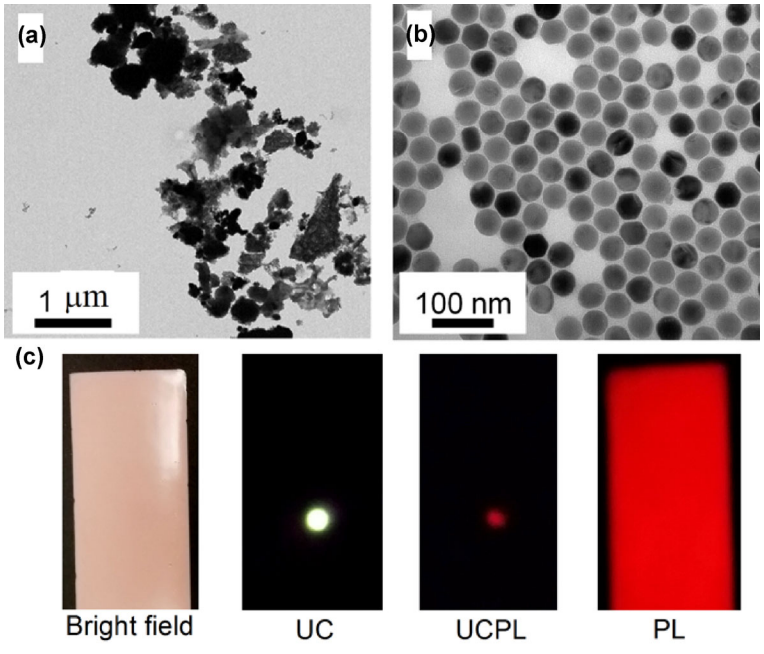

Figure 1 TEM images of the as-synthesized (a) CaS:Eu,Tm,Ce nanoparticles, (b) β-$NaYF_4$:20%Yb,2%Er/$NaYF_4$ nanoparticles, and (c) digital pictures of the as-synthesized UCPL membrane taken by an iPhone 6 camera, from left to right: under room-light, under 980 nm CW laser (468 mW/cm^2) irradiation in the dark, afterglow image after turning off the laser, and afterglow after white LED irradiation.

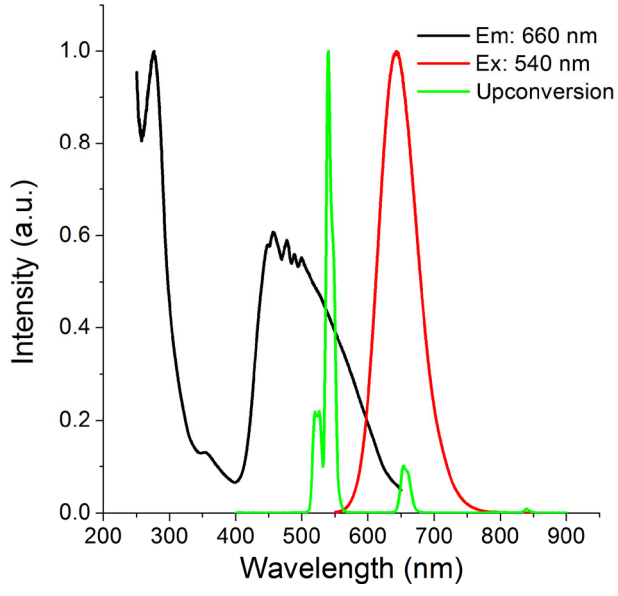

Figure 2 Persistent luminescence excitation spectrum (black line, monitored at the emission of 660 nm) and emission spectrum (red line, excited at 540 nm) of CaS:0.02%Eu,0.1%Tm,0.1%Ce, shown with the upconversion luminescence spectrum (green line, excited by 980 nm laser irradiation) of standard, β-$NaYF_4$:20%Yb,2%Er/$NaYF_4$ UCNPs.

membrane under a series of excitation power densities. Under 980 nm laser irradiation, in addition to typical UC luminescence from β-$NaYF_4$:20%Yb,2%Er/$NaYF_4$, we found broad shoulder peaks between 580 to 650 nm, which can be assigned to the luminescence spectra of Eu^{2+} in CaS [39, 40]. Figure 3(b) shows the PL spectra of the film after turning off the NIR laser irradiation. We observed that the PL emission could be activated under a power density as low as 145 mW/cm^2. Furthermore, a short exposure time (10 s) was used to generate efficient PL emission. The PL intensity increased with higher exposure power density, implying that the exposure time can be shortened by increasing the power density. Figure 3(c) shows the PL decay curves from 980 nm laser excitation. It shows decay profiles typical for persistent phosphors. Notably, the PL can be completely reactivated at any time using NIR irradiation (Fig. 3(d)).

The as-synthesized UCPL film has potential applications in luminescence bioimaging. As a proof of concept, a small piece of the UCPL membrane (1 mm × 2 mm) was implanted into the thigh of a mouse to model a medical implant. As indicated in Fig. 4(a), this membrane can be activated by room light during surgery. Since the PL signal became relatively weak 20 min after implant, a 980 nm NIR laser (468 mW/cm^2) was utilized to reactivate the PL of the device *in vivo* and *in situ*. The reactivated PL kept decaying for

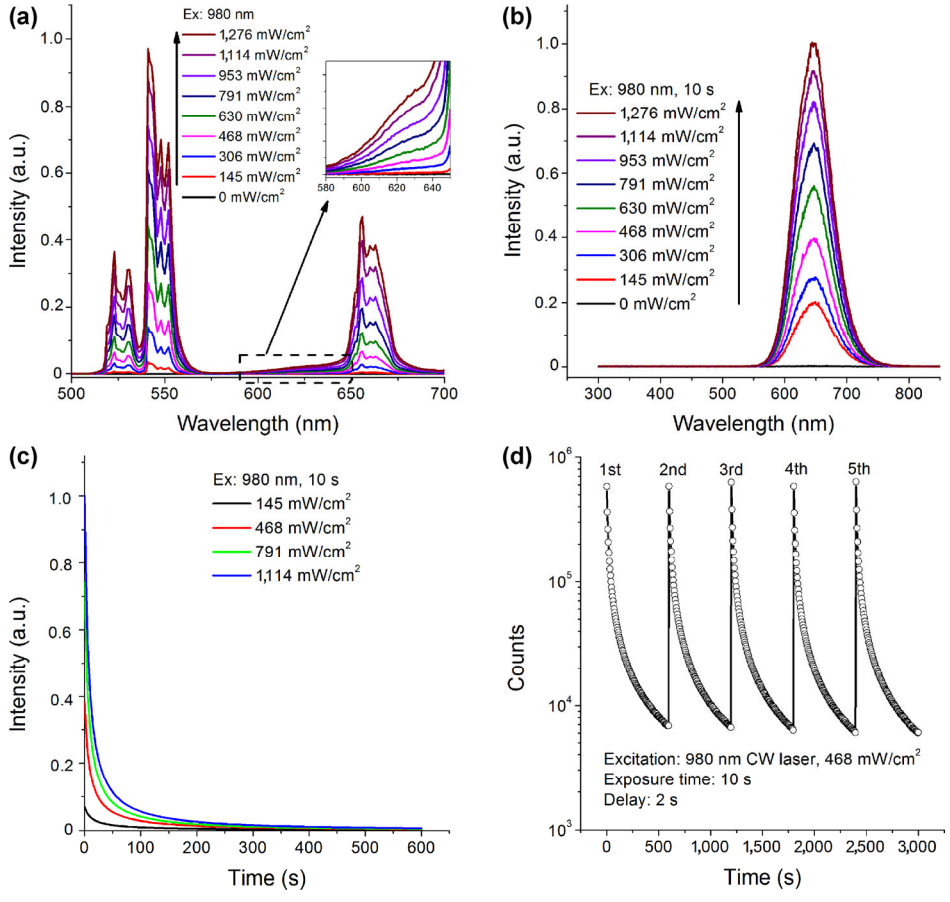

Figure 3 Spectral properties of the as-prepared UCPL composite membrane. (a) UC luminescence spectra of the UCPL membrane under 980 nm constant wave laser irradiation. (b) PL spectra 10 s after turning off the NIR laser. (c) PL decay curves after exposure to various power densities. (d) Repeatable NIR-excitation/red-PL-emission decay curves recorded at 640 nm.

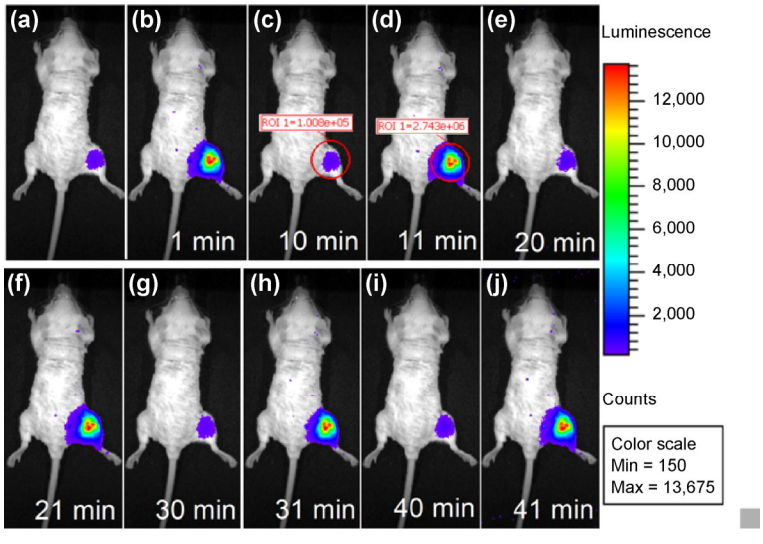

Figure 4 PL imaging of a UCPL membrane device (1 mm × 2 mm) implanted into the thigh of a mouse. The image in (a) was taken 20 min after the device was transplanted, the PL signal likely stems from exposure to room-light during the surgery. Images in (b), (d), (f), (h), and (j) were taken 1 min after 980 nm laser exposure for 10 s. Images in (c), (e), (g), and (i) were taken 10 min after laser irradiation ceased. An ROI tool was utilized to analyze the luminescence intensity of selected areas. The ROI values in (c) and (d) are 1.008×10^5 and 2.743×10^6, respectively. The imaging settings here are: exposure 5 s, bin 4, f/stop 1, no filter and the CW NIR laser exposure was 468 mW/cm^2, for 10 s.

~10 min. It should be noted that the imaging time window could be further extended by increasing the exposure time (Fig. S2 in the ESM). The reactivation could be replicated multiple times with a stable PL intensity (also shown in Fig. S3 in the ESM), meaning that one can reactivate the PL emission at any time if needed by using a 980 nm NIR laser and PLNPs can indeed be reactivated in conjugation with UCNPs. In comparison with traditional UC luminescence imaging, UCPL imaging is simpler to process. The UC laser excitation is conducted before the PL imaging and can thus be performed using traditional luminescence imaging systems without any equipment modification like laser control. Further, UCPL imaging potentially has less heating effects than traditional UC biomedical processes. The excited PL can last for long periods after several seconds of excitation. Such short laser exposure times will alleviate the potential health risks of laser therapy, especially in cases where long-term light exposure is needed.

3 Conclusions

We successfully fabricated a UCPL system by simply integrating UCNPs and PLNPs together. This system possesses both intense UC and PL properties derived from standard β-$NaYF_4$:Yb,Er@$NaYF_4$ upconversion NPs and CaS:Eu,Tm,Ce deep red persistent luminescence NPs, respectively. We confirm that the red persistent luminescence of PLNPs can be repeatedly activated by NIR via UCNPs both *in vitro* and *in vivo*. Although this UCPL system is a simple mixture of two different nanoparticles, we believe it can be improved by fabricating novel compact nanosystems such as core/shell nanostructures. Generally, our result provides a novel understanding of the fabrication of UCPL functional materials and their potential applications in UCPL imaging, deep tissue photodynamic therapy, and optogenetics, etc. [41, 42]. This research should also facilitate the further development of PLNPs in photonics and biophotonics.

Acknowledgements

This research was supported by the start-up fund of the University of Massachusetts Medical School, a Worcester Foundation Mel Cutler Award, the National Institute of Health R01MH103133, the Human Frontier Science Program, a UMass CVIP award, and a UMass OCTV award.

Electronic Supplementary Material: Supplementary material (the experimental details, comparative PL decay curves of CaS:Eu,Tm,Ce vs. $ZnGa_2O_4$:Cr excited by 540 nm irradiation, and UCPL imaging obtained using diverse exposure settings) is available in the online version of this article at http://dx.doi.org/10.1007/s12274-017-1548-9.

References

[1] van den Eeckhout, K.; Smet, P. F.; Poelman, D. Persistent luminescence in Eu^{2+}-doped compounds: A review. *Materials* **2010**, *3*, 2536–2566.

[2] Li, Y.; Gecevicius, M.; Qiu, J. R. Long persistent phosphors-from fundamentals to applications. *Chem. Soc. Rev.* **2016**, *45*, 2090–2136.

[3] le Masne de Chermont, Q.; Chaneac, C.; Seguin, J.; Pelle, F.; Maitrejean, S.; Jolivet, J. P.; Gourier, D.; Bessodes, M.; Scherman, D. Nanoprobes with near-infrared persistent luminescence for *in vivo* imaging. *Proc. Natl. Acad. Sci. USA* **2007**, *104*, 9266–9271.

[4] Liang, Y. J.; Liu, F.; Chen, Y. F.; Sun, K. N.; Pan, Z. W. Long persistent luminescence in the ultraviolet in Pb^{2+}-doped $Sr_2MgGe_2O_7$ persistent phosphor. *Dalton Trans.* **2016**, *45*, 1322–1326.

[5] Liu, F.; Liang, Y. J.; Chen, Y. F.; Pan, Z. W. Divalent nickel-activated gallate-based persistent phosphors in the short-wave infrared. *Adv. Opt. Mater.* **2016**, *4*, 562–566.

[6] Li, Y.; Li, Y. Y.; Chen, R. C.; Sharafudeen, K.; Zhou, S. F.; Gecevicius, M.; Wang, H. H.; Dong, G. P.; Wu, Y. L.; Qin, X. X. et al. Tailoring of the trap distribution and crystal field in Cr^{3+}-doped non-gallate phosphors with near-infrared long-persistence phosphorescence. *NPG Asia Mater.* **2015**, *7*, e180.

[7] Xu, J.; Ueda, J.; Kuroishi, K.; Tanabe, S. Fabrication of Ce^{3+}-Cr^{3+} co-doped yttrium aluminium gallium garnet transparent ceramic phosphors with super long persistent luminescence. *Scr. Mater.* **2015**, *102*, 47–50.

[8] Jin, Y. H.; Hu, Y. H.; Chen, L.; Ju, G. F.; Wu, H. Y.; Mu, Z. F.; He, M.; Xue, F. H. Luminescent properties of a green long persistent phosphor Li_2MgGeO_4:Mn^{2+}. *Opt. Mater. Express* **2016**, *6*, 929–937.

[9] Kong, J. T.; Zheng, W.; Liu, Y. S.; Li, R. F.; Ma, E.; Zhu, H. M.; Chen, X. Y. Persistent luminescence from Eu^{3+} in SnO_2 nanoparticles. *Nanoscale* **2015**, *7*, 11048–11054.

[10] Guo, H. J.; Wang, Y. H.; Chen, W. B.; Zeng, W.; Han, S. C.; Li, G.; Li, Y. Y. Controlling and revealing the trap distributions of $Ca_6BaP_4O_{17}$:Eu^{2+}, R^{3+} (R = Dy, Tb, Ce, Gd, Nd) by codoping different trivalent lanthanides. *J. Mater. Chem. C* **2015**, *3*, 11212–11218.

[11] Bessière, A.; Lecointre, A.; Benhamou, R. A.; Suard, E.; Wallez, G.; Viana, B. How to induce red persistent luminescence in biocompatible $Ca_3(PO_4)_2$. *J. Mater. Chem. C* **2013**, *1*, 1252–1259.

[12] Palner, M.; Pu, K. Y.; Shao, S.; Rao, J. H. Semiconducting polymer nanoparticles with persistent near-infrared luminescence for *in vivo* optical imaging. *Angew. Chem., Int. Ed.* **2015**, *54*, 11477–11480.

[13] Abdukayum, A.; Chen, J. T.; Zhao, Q.; Yan, X. P. Functional near infrared-emitting Cr^{3+}/Pr^{3+} co-doped zinc gallogermanate persistent luminescent nanoparticles with superlong afterglow for *in vivo* targeted bioimaging. *J. Am. Chem. Soc.* **2013**, *135*, 14125–14133.

[14] Maldiney, T.; Doan, B. T.; Alloyeau, D.; Bessodes, M.; Scherman, D.; Richard, C. Gadolinium-doped persistent nanophosphors as versatile tool for multimodal *in vivo* imaging. *Adv. Funct. Mater.* **2015**, *25*, 331–338.

[15] Abdukayum, A.; Yang, C. X.; Zhao, Q.; Chen, J. T.; Dong, L. X.; Yan, X. P. Gadolinium complexes functionalized persistent luminescent nanoparticles as a multimodal probe for near-infrared luminescence and magnetic resonance imaging *in vivo*. *Anal. Chem.* **2014**, *86*, 4096–4101.

[16] Dai, W. B.; Lei, Y. F.; Ye, S.; Song, E. H.; Chen, Z.; Zhang, Q. Y. Mesoporous nanoparticles Gd_2O_3@$mSiO_2$/$ZnGa_2O_4$:Cr^{3+},Bi^{3+} as multifunctional probes for bioimaging. *J. Mater. Chem. B* **2016**, *4*, 1842–1852.

[17] Shi, J. P.; Sun, X.; Li, J. L.; Man, H. Z.; Shen, J. S.; Yu, Y. K.; Zhang, H. W. Multifunctional near infrared-emitting long-persistence luminescent nanoprobes for drug delivery and targeted tumor imaging. *Biomaterials* **2015**, *37*, 260–270.

[18] Wu, S. Q.; Chi, C. W.; Yang, C. X.; Yan, X. P. Penetrating peptide-bioconjugated persistent nanophosphors for long-term tracking of adipose-derived stem cells with superior signal-to-noise ratio. *Anal. Chem.* **2016**, *88*, 4114–4121.

[19] Zhang, L.; Lei, J. P.; Liu, J. T.; Ma, F. J.; Ju, H. X. Persistent luminescence nanoprobe for biosensing and lifetime imaging of cell apoptosis via time-resolved fluorescence resonance energy transfer. *Biomaterials* **2015**, *67*, 323–334.

[20] Tang, Y. R.; Song, H. J.; Su, Y. Y.; Lv, Y. Turn-on persistent luminescence probe based on graphitic carbon nitride for imaging detection of biothiols in biological fluids. *Anal. Chem.* **2013**, *85*, 11876–11884.

[21] Tang, J.; Su, Y. Y.; Deng, D. Y.; Zhang, L. C.; Yang, N.; Lv, Y. A persistent luminescence microsphere-based probe for convenient imaging analysis of dopamine. *Analyst* **2016**, *141*, 5366–5373.

[22] Chuang, Y. J.; Liu, F.; Wang, W.; Kanj, M. Y.; Poitzsch, M. E.; Pan, Z. W. Ultra-sensitive *in-situ* detection of near-infrared persistent luminescent tracer nanoagents in crude oil-water mixtures. *Sci. Rep.* **2016**, *6*, 27993.

[23] Liu, F.; Yan, W. Z.; Chuang, Y. J.; Zhen, Z. P.; Xie, J.; Pan, Z. W. Photostimulated near-infrared persistent luminescence as a new optical read-out from Cr^{3+}-doped $LiGa_5O_8$. *Sci. Rep.* **2013**, *3*, 1554.

[24] Maldiney, T.; Bessière, A.; Seguin, J.; Teston, E.; Sharma, S. K.; Viana, B.; Bos, A. J. J.; Dorenbos, P.; Bessodes, M.; Gourier, D. et al. The *in vivo* activation of persistent nanophosphors for optical imaging of vascularization, tumours and grafted cells. *Nat. Mater.* **2014**, *13*, 418–426.

[25] Li, Z. J.; Zhang, Y. W.; Wu, X.; Wu, X. Q.; Maudgal, R.; Zhang, H. W.; Han, G. *In vivo* repeatedly charging near-infrared-emitting mesoporous SiO_2/$ZnGa_2O_4$:Cr^{3+} persistent luminescence nanocomposites. *Adv. Sci.* **2015**, *2*, 1500001.

[26] Li, Z. J.; Zhang, Y. W.; Wu, X.; Huang, L.; Li, D. S.; Fan, W.; Han, G. Direct aqueous-phase synthesis of sub-10 nm "luminous pearls" with enhanced *in vivo* renewable near-infrared persistent luminescence. *J. Am. Chem. Soc.* **2015**, *137*, 5304–5307.

[27] Bessière, A.; Jacquart, S.; Priolkar, K.; Lecointre, A.; Viana, B.; Gourier, D. $ZnGa_2O_4$:Cr^{3+}: A new red long-lasting phosphor with high brightness. *Opt. Express* **2011**, *19*, 10131–10137.

[28] Zhuang, Y. X.; Ueda, J.; Tanabe, S. Enhancement of red persistent luminescence in Cr^{3+}-doped $ZnGa_2O_4$ phosphors by Bi_2O_3 codoping. *Appl. Phys. Express* **2013**, *6*, 052602.

[29] Zhuang, Y. X.; Ueda, J.; Tanabe, S. Tunable trap depth in $Zn(Ga_{1-x}Al_x)_2O_4$:Cr,Bi red persistent phosphors: Considerations of high-temperature persistent luminescence and photostimulated persistent luminescence. *J. Mater. Chem. C* **2013**, *1*, 7849–7855.

[30] Pan, Z. W.; Lu, Y. Y.; Liu, F. Sunlight-activated long-persistent luminescence in the near-infrared from Cr^{3+}-doped zinc gallogermanates. *Nat. Mater.* **2012**, *11*, 58–63.

[31] Liu, F.; Liang, Y. J.; Pan, Z. W. Detection of up-converted persistent luminescence in the near infrared emitted by the $Zn_3Ga_2GeO_8$:Cr^{3+},Yb^{3+},Er^{3+} phosphor. *Phys. Rev. Lett.* **2014**, *113*, 177401.

[32] Li, Z. J.; Zhang, Y. W.; La, H. E.; Zhu, R.; El-Banna, G.; Wei, Y. Z.; Han, G. Upconverting NIR photons for bioimaging. *Nanomaterials* **2015**, *5*, 2148–2168.

[33] Chen, X.; Peng, D. F.; Ju, Q.; Wang, F. Photon upconversion in core–shell nanoparticles. *Chem. Soc. Rev.* **2015**, *44*, 1318–1330.

[34] Idris, N. M.; Jayakumar, M. K. G.; Bansal, A.; Zhang, Y. Upconversion nanoparticles as versatile light nanotransducers for photoactivation applications. *Chem. Soc. Rev.* **2015**, *44*, 1449–1478.

[35] Wu, X. M.; Zhu, W. H. Stability enhancement of fluorophores for lighting up practical application in bioimaging. *Chem. Soc. Rev.* **2015**, *44*, 4179–4184.

[36] Jia, D. D. Enhancement of long-persistence by Ce co-doping in CaS:Eu^{2+},Tm^{3+} red phosphor. *J. Electrochem. Soc.* **2006**, *153*, H198–H201.

[37] Wu, X.; Zhang, Y. W.; Takle, K.; Bilsel, O.; Li, Z. J.; Lee, H.; Zhang, Z. J.; Li, D. S.; Fan, W.; Duan, C. Y. et al. Dye-sensitized core/active shell upconversion nanoparticles for optogenetics and bioimaging applications. *ACS Nano* **2016**, *10*, 1060–1066.

[38] Van Haecke, J. E.; Smet, P. F.; De Keyser, K.; Poelman, D. Single crystal CaS:Eu and SrS:Eu luminescent particles obtained by solvothermal synthesis. *J. Electrochem. Soc.* **2007**, *154*, J278–J282.

[39] Rodríguez Burbano, D. C.; Sharma, S. K.; Dorenbos, P.; Viana, B.; Capobianco, J. A. Persistent and photostimulated red emission in CaS:Eu^{2+},Dy^{3+} nanophosphors. *Adv. Opt. Mater.* **2015**, *3*, 551–557.

[40] Guo, C. F.; Huang, D. X.; Su, Q. Methods to improve the fluorescence intensity of CaS:Eu^{2+} red-emitting phosphor for white LED. *Mater. Sci. Eng. B* **2006**, *130*, 189–193.

[41] Sakdinawat, A.; Attwood, D. Nanoscale X-ray imaging. *Nat. Photonics* **2010**, *4*, 840–848.

[42] Grayson, W. L.; Bunnell, B. A.; Martin, E.; Frazier, T.; Hung, B. P.; Gimble, J. M. Stromal cells and stem cells in clinical bone regeneration. *Nat. Rev. Endocrinol.* **2015**, *11*, 140–150.